

IFSCC 2025 full paper (IFSCC2025-1456)

“Preparation of supramolecular BR-LicoA-VE for promoting permeability and whitening effects”

Tao Zhang^{1,*}, Beibei Lu², Yue Liu¹, Xuefang Shi¹, Yimeng Wang¹, Bo Ruan², and Jiaheng Zhang²

¹Better Way (Shanghai) Cosmetics Co. Ltd. Shanghai 200233, P.R. China.;

²Shenzhen Shinehigh Innovation Technology Co., Ltd. Shenzhen 518055, P. R. China.

Abstract

As people age and are exposed to the sun for a long time, the excessive production and accumulation of melanin in the skin can affect their appearance and health. 4-Butylresorcinol (BR) can achieve the goal of whitening and lightening spots by inhibiting the activity of tyrosinase (TYR) and dihydroxyindole carboxylate oxidase. However, the high irritancy of BR limits its application. Therefore, we prepared supramolecules of BR, licochalcone A (LicoA), and vitamin E acetate (VE) through intermolecular forces. Among them, the combination of BR and LicoA is to reduce the irritation of BR, while the addition of VE is to improve skin permeability. The supramolecular BR-LicoA-VE exhibits good skin permeability and stability at room temperature. The supramolecular BR-LicoA-VE can significantly reduce the melanin content of the skin (30.55%) and inhibit the activity of TYR (59.90%). At the same time, the addition of LicoA to the supramolecular design of BR-LicoA-VE greatly improves the photostability of BR, overcoming the disadvantage of poor photostability of traditional whitening ingredients. Through simulation calculations, it was found that supramolecular BR-LicoA-VE can inhibit the production of melanin in cells by suppressing the expression of melanin-related proteins such as TYR, endothelin-1, mammalian target of rapamycin, and microphthalmia-associated transcription factor. In the clinical trials, a formula containing supramolecular BR-LicoA-VE shows better skin whitening efficacy compared with the BR and phenylethyl resorcinol groups, with the melanin being the lowest and the whiteness value the highest. The decrease of a value indicates that the formula with supramolecular BR-LicoA-VE can also decrease a value indicating that it may have the potential for soothing potential effect. Therefore, supramolecular BR-LicoA-VE has potential application value in whitening and skincare.

1. Introduction

In recent years, whitening is a rapidly developing category, the demand for whitening products has gradually shifted from whitening and reducing pigmentation to early prevention and care [1, 2]. Therefore, many cosmetic companies have conducted extensive research in the field of whitening, committed to developing whitening products with high efficacy, high stability, and low irritation.

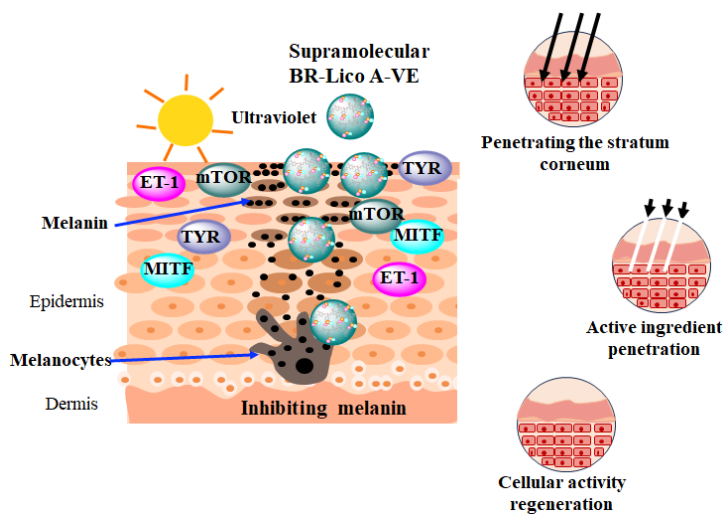
Melanin is an important factor affecting human skin color, and a large amount of melanin accumulation will eventually lead to freckles and melasma [3]. In recently, multiple approaches

and perspectives have been developed for whitening strategies, including prevention of exogenous stimulation, inhibition of related enzyme activity, and improvement of the stratum corneum metabolic rate [6].

Among various whitening strategies, inhibiting the formation of melanin is the most important pathway [5]. 4-Butylresorcinol (BR) mainly achieves the purpose of whitening and lightening spots by inhibiting the activities of tyrosinase (TYR) and dihydroxyindole carboxylate oxidase [6]. BR has excellent tyrosinase inhibitory activity, and its safety performance is higher than that of other resorcinol raw materials [7]. Licochalcone A (LicoA) is a highly active ingredient extracted from licorice, which has excellent inhibitory effects on inflammatory factors and significant antibacterial effects and inhibit the activity of endothelin-1 (ET-1), thereby inhibiting the formation of melanin [8].

Supramolecular molecules have a wide range of applications in fields such as medicine, biology, and food [9, 10]. The addition of supramolecules can not only solve the irritancy of BR but also improve its permeability and stability.

Based on the stability, compatibility, and action of raw materials, the whitener mainly composed of BR and LicoA was selected. LicoA can reduce the irritation of BR and improve its stability. VE can synergistically assist in improving the skin permeability of BR and LicoA and also help stabilize BR. Therefore, through a combination of theoretical calculation and experiment, BR, LicoA, and VE were combined to form supramolecules through intermolecular forces. This supramolecule BR-LicoA-VE has good stability, can significantly reduce melanin content, and has good whitening effects (better than 577 and 377 groups). Through simulation calculations, it was found that supramolecular BR-LicoA-VE can inhibit the production of melanin in cells by suppressing the expression of melanin-related proteins such as TYR, ET-1, mammalian target of rapamycin (mTOR), and microphthalmia-associated transcription factor (MITF). Therefore, the supramolecular 577 transdermal drug delivery nanocarrier technology can achieve synergistic enhancement of whitening ingredients with different mechanisms of action (Scheme 1).



Scheme 1. Schematic diagram illustrating supramolecular BR-LicoA-VE can not only open skin channels to deliver active ingredients and activate the cell regeneration, but also inhibit the generation of melanocytes by regulating the expression of TYR, ET-1, mTOR, and MITF, thereby achieving skin whitening.

2. Materials and Methods

2.1 Reagents

4-butyl resorcinol (BR, 577) was purchased from Clariant Chemicals (China) Ltd. (Shanghai, China), phenylethyl resorcinol (PR, 377) was purchased from Symrise (China) Ltd. Licochalcone A (LicoA) was purchased from Qinghai Lake Pharmaceutical Co., Ltd (Qinghai, China). Vitamin E acetate (VE) was purchased from BASF (China) Co., Ltd (Shanghai, China). Pig abdominal skin was stored at -80°C and thawed immediately before use. MTT kits were purchased from Beyotime Biotechnology (Shanghai, China). Dulbecco's modified Eagle Medium (DMEM), fetal bovine serum (FBS), and pancreatic enzymes were obtained from Gibco (Grand Island, NY, USA). Fluorescein isothiocyanate (FITC) was purchased from Dalian Meilun Biotechnology Co., Ltd (Liaoning, China).

2.2 Characterization of supramolecular BR-LicoA-VE

The chemical structures of the supramolecular BR-LicoA-VE dispersed in DMSO-d₆ were analyzed by proton nuclear magnetic resonance (1H NMR) spectroscopy (Bruker Avance III 400, USA) and FTIR spectroscopy (Thermo Scientific Nicolet iS 50, USA). The morphology of the supramolecular BR-LicoA-VE was observed using transmission electron microscopy (TEM, 300 kV, FEI Talos Arctica, USA). Thermogravimetric analysis (TGA) was performed using N₂ with a temperature increment of 10 °C min⁻¹ on a thermal analyzer (NETZSCH STA 449F3, Germany). Differential scanning calorimetry (DSC) measurements were performed with N₂ as the purge gas, and the system was cooled using liquid nitrogen with a temperature increment of 10 °C min⁻¹ on a thermal analyzer (Mettler Toledo DSC3, Switzerland). The size and zeta potential of the supramolecular BR-LicoA-VE were measured by dynamic light scattering (DLS) using Zetasizer Nano ZS (Malvern, UK). High-performance liquid chromatography (HPLC) was performed using an Agilent 1100 equipped (Agilent, Santa Clara, USA). The CM-26dG spectrophotometer (KONICA MINOLTA, Japan) was used to detect the skin color. The Mexame-ter® MX 18 (Courage + Khazaka, Germany) was used to detect the melanin and erythema levels of the skin. The Tewameter® TM Hex (Courage + Khazaka, Germany) was used to detect the transdermal water loss (TEWL) of the skin.

2.3 Preparation of supramolecular BR-LicoA-VE

Take 5 g of BR (0.03 mol) and 1 g of LicoA (0.003 mol), add 20 mL of ethanol solvent, and start stirring at a speed of 300 rpm and 40 °C. Dissolve BR and LicoA were completely dissolved to obtain a clarified solution. Take another container, weigh 8 g (0.017 mol) of VE, add 20 mL of ethanol, and stir until VE is completely dissolved. Maintain the stirring speed and stirring temperature constant in the reactor, and add VE dropwise to the solution containing BR and LicoA to induce a supramolecular modification reaction between BR and LicoA with VE. The reaction time was 20 h. After the reaction was complete, the solution was slowly cooled to room temperature, and a rotary evaporator was used to remove the solvent. Then add an appropriate amount of ethanol-water for recrystallization, remove the solvent with a rotary evaporator, and finally collect the liquid. It was dried in a vacuum oven at 40 °C for 24 h and was named supramolecular BR-LicoA-VE.

2.4 Preparation of supramolecular BR-LicoA-VE-FITC

Briefly, 2 mL of fluorescein isothiocyanate (FITC) solution (2.5 mg mL⁻¹) was added to 3 mL supramolecular BR-LicoA-VE, and the pH of the solution was adjusted to neutral using sodium hydroxide. The FITC-loaded supramolecular BR-LicoA-VE was obtained after vigorous stirring in the dark overnight and was named supramolecular BR-LicoA-VE-FITC after dialysis.

2.5 In vitro skin penetration of supramolecular BR-LicoA-VE

The clean pig abdominal skin was fixed between the diffusion and receiving chambers, the receiving chamber was filled with 0.01 M PBS. The magnetic stirring speed was set at 350 r min⁻¹, and the water bath temperature was 32 ± 1 °C. Then, 0.5 mL of supramolecule BR-LicoA-VE (1.0 mg mL⁻¹) was added to the diffusion chamber. At different time points, take 1 mL of the receiving solution (V₀) and add the same volume of fresh receiving solution. After

the experiment, the cumulative permeability of the supramolecular BR-LicoA-VE in each layer of the skin was detected by high-performance liquid chromatography (HPLC).

2.6 In vitro cytotoxicity

The melanin cells were incubated in a 96-well plate at a density of 5000 cells/well, and cultured for 24 h. Discard the culture medium and add 100 µL supramolecular BR-LicoA-VE for incubation 24 h, adding 10 µL MTT reagent for another 4 h. Subsequently, add 150 µL DMSO, shake for 10 min, and measure at 490 nm using a microplate reader (BioTek, Gen5, USA). Finally, the cell survival rate was calculated using the formula.

2.7 3D melanin model (MelaKutis®) testing

Add 3.7mL of melanin model culture medium to each well on a 6-well plate, and transfer the model received on the day (day 0) to the labeled 6-well plate. Starting from day 0 of the model, experiment groups were subjected to UVB irradiation treatment daily (50 mJ/cm²), while the blank control group was not subjected to UVB irradiation. The positive group (kojic acid) and the sample group were administered twice on day 3 and day 5, respectively, using surface administration with a volume of 2 mg/cm². After 7 days, collect the sample for testing. After the model cultivation was completed, first use a camera to take epigenetic photos. Next, perform apparent brightness (L* value) detection on the model after the apparent chromaticity detection is completed. Finally, the model with L* value detection is placed in a clean centrifuge tube for melanin content determination.

2.8 Testing of melanin content based on melanocytes

Inoculate melanin cells into a 6-well plate. After completion of administration, place in incubator for 72 h. Then use a digestion cell to collect and centrifuge the cells, and discard the supernatant. Then 200 µL distilled water, 500 µL anhydrous ethanol, and 500 µL ether were added to the centrifuge tube successively. After being thoroughly mixed, the centrifuge was left at room temperature for 20 min, 3000 r/min for 5 min, and the supernatant was discarded. Add 1 mL NaOH aqueous solution (1 mol/L) containing 10% DMSO and heat in an 80 °C water bath for 40 min. After the hot incubation was completed, take 200 µL of the supernatant and transfer it into a 96-well plate to measure the optical density value at 405 nm.

2.9 Tyrosinase inhibition rate and dendritic cell morphology test method

Inoculated melanin cells into a 6-well plate. After administration, the 6-well plates were placed in a CO₂ incubator for 24 h. After incubation, take photos under a microscope. The cells were then collected, centrifuged, and lysed with 0.5% sodium deoxycholate, then centrifuged and the supernatant was collected. Protein quantification was performed on all samples according to the bicinchoninic acid kit instructions. Finally, the samples were added to a centrifuge tube at 90 µL and each tube was added with 10 µL levodopa (0.1%). The absorbance values of each sample were read at 475 nm and the inhibition rate of tyrosinase was calculated.

2.10 Safety evaluation

According to the "Technical Specifications for the Safety of Cosmetics (2015 Edition)", a cosmetics patch test on the human body was carried out. Thirty-four healthy volunteers aged 21-59 years with no history of skin diseases or allergies were selected. Skin reactions were observed and recorded at 0.5 h, 24 h, and 48 h after the spot tester was removed, according to the skin reaction grading standard. Cosmetic formula containing BR-LicoA-VE, BR, PR and no whitening agent were prepared for testing.

2.11 Evaluation of the whitening, soothing, and repairing effects

48 healthy subjects (aged 23-50) were recruited. Under normal circumstances, subjects use the test product according to the instructions for 28 days to evaluate its whitening, soothing, and repairing effects.

Whitening evaluation methods

Improve skin melanin or skin color. The MI value and ITA° value are suitable parameters for evaluating the efficacy of functional cosmetics. The smaller the MI value, the less the skin melanin content. The larger the ITA° value, the brighter the skin color . A positioning card is used to accurately determine the test location, ensuring that the test positions remain consistent across multiple time points.

Repair evaluation methods

Improvement of skin transcutaneous water loss rate (TEWL). The TEWL value is a suitable parameter for assessing the effectiveness of functional cosmetics. The smaller the TEWL value, the better the skin barrier. A positioning card is used to accurately determine the test location, ensuring that the test positions remain consistent across multiple time points.

Soothing evaluation methods

Improvement of skin erythema.The EI value is a suitable parameter for assessing the effectiveness of functional cosmetics. The smaller the EI value, the less red the skin. A positioning card is used to accurately determine the test location, ensuring that the test positions remain consistent across multiple time points.

2.12 Theoretical calculation methods

Gaussian 09 software was used for the optimal configurations, vibrational frequency calculations, and electrostatic potential (ESP) analysis [11, 12]. Multiwfn and Winvmd programs were used for reduce density gradient (RDG) analysis. AlphaFold2 was used for modeling to obtain the three-dimensional structure of the protein. Molecular docking between supramolecular and proteins was performed using AutoDock 4.2.6 software.

2.13 Statistical analysis

All results are expressed as mean \pm standard deviation. Statistical significance was set at * p < 0.05, ** p < 0.01, and *** p < 0.001.

3. Results

3.1 Synthesis, optimization, and characterization of supramolecular BR-LicoA-VE

BR, LicoA, and VE can form supramolecular BR-LicoA-VE through intermolecular forces. From the NMR spectra, the chemical shift of supramolecular BR-LicoA-VE has undergone significant changes compared to monomers BR, LicoA, and VE. These chemical shifts indicate that the supramolecular BR-LicoA-VE was formed through intermolecular forces [13, 14]. Therefore, NMR and FTIR spectra indicated that the supramolecular BR-LicoA-VE has been successfully prepared. In addition, supramolecular BR-LicoA-VE has good thermal stability [15].

BR, LicoA, and VE can self-assemble into supramolecules through intermolecular forces (Figure 1a). The surface electrostatic potential (ESP) diagram of the supramolecule BR-LicoA-VE can be simulated using density functional theory. The depth of the color in the diagram reflects the magnitude of the surface electrostatic potential, with red indicating a positive electrostatic potential and blue indicating a negative surface electrostatic potential. From the ESP diagram (Figure 1b), it can be seen that during the formation of supramolecular BR-LicoA-VE, BR approaches, LicoA, and VE. Therefore, calculations indicate that supramolecule BR-LicoA-VE can stably exist at room temperature. The density gradient graph (RDG) of supramolecular BR-LicoA-VE shows that blue represents strong attractive interactions (such as electrostatic interactions caused by hydrogen bonding), while red represents strong unbound overlaps, and the transition zone represents typical van der Waals interactions, including dipole, dispersion, and hydrophobic interactions. From the figure (Figure 1c), the transition region between BR, LicoA, and VE shows two large flakes, indicating the presence of van der Waals interactions in the monomer of supramolecular BR-LicoA-VE during structural formation, which contributes to the formation of supramolecules [16]. The supramolecular BR-LicoA-VE appears as small

spherical particles in the solution, with a particle size of 18.26 nm and uniform distribution in the solution. The storage of supramolecular BR-LicoA-VE in solution for 28 days did not show significant changes, indicating that supramolecular BR-LicoA-VE has good solubility stability. The potential of supramolecular BR-LicoA-VE was 28.37mV, indicating that the distribution of supramolecular BR-LicoA-VE was uniform, which is beneficial for skin penetration, and has potential application value in the field of cosmetics [17].

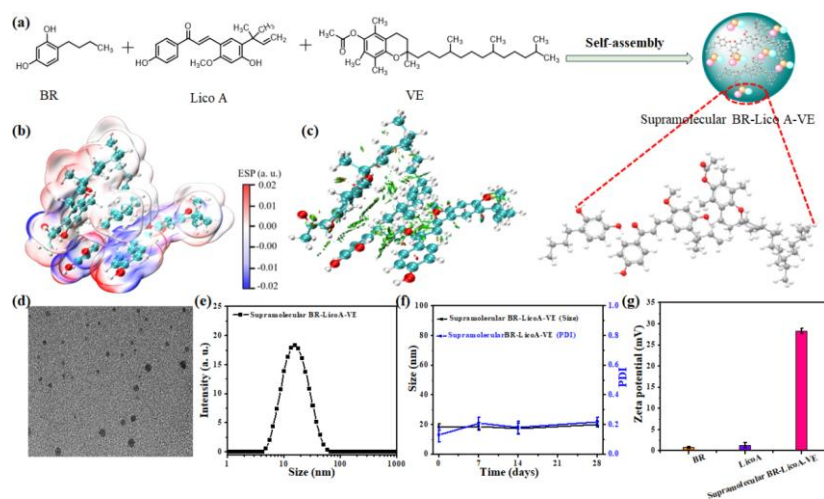


Figure 1. Characterization of supramolecular BR-LicoA-VE. (a) Schematic diagram of the preparation process of supramolecular BR-LicoA-VE. (b) ESP diagram and (c) RDG diagram of supramolecular BR-LicoA-VE. (d) TEM image of supramolecular BR-LicoA-VE in solution, (e) particle size image, (f) stability image, and (i) zeta potential images ($n=3$).

3.2 Transdermal delivery of supramolecular BR-LicoA-VE

The schematic diagram of the permeation of supramolecular BR-LicoA-VE (Figure 2a) shows that the supramolecular BR-LicoA-VE first penetrates the stratum corneum, and the active ingredients pass through the cells for intracellular permeation and absorption, followed by activation of the expression of the active ingredients within the cells [18]. With the increase of time, the transdermal penetration of supramolecular BR-LicoA-VE gradually increases until reaching an equilibrium state. After 24 h of penetration, the cumulative penetration of BR in supramolecular BR-LicoA-VE was 2.70 times that of BR (Figure 2b), and the cumulative penetration of LicoA in supramolecular BR-LicoA-VE was 2.37 times that of LicoA (Figure 2c). The fluorescence pattern of supramolecular BR-LicoA-VE after percutaneous penetration for 24 h also showed (Figure 2d) that supramolecular BR-LicoA-VE can penetrate the stratum corneum and deliver the active ingredients BR and LicoA to the epidermis and dermis of the skin, thereby exerting corresponding effects.

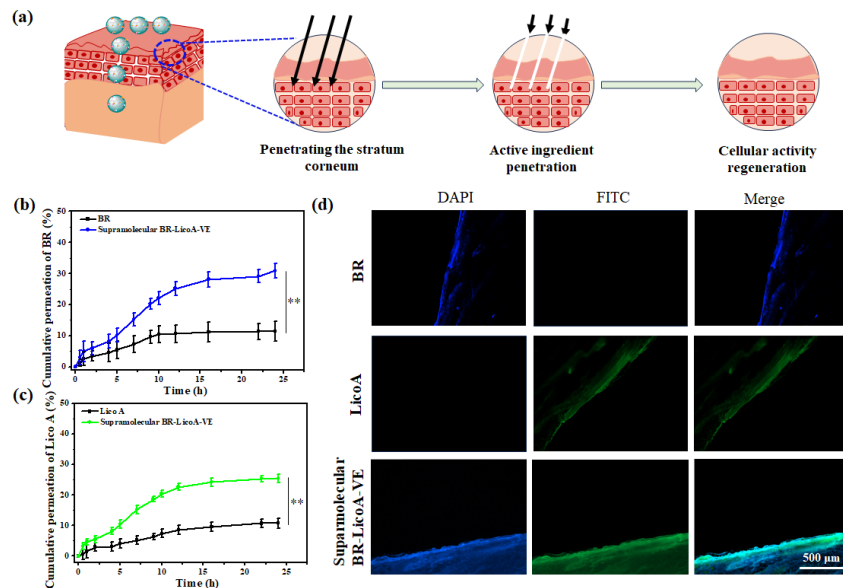


Figure 2. Skin permeability and mechanism of supramolecular BR-LicoA-VE. (a) The scheme of supramolecular BR-LicoA-VE percutaneous penetration. (b) The cumulative amount of BR percutaneous penetration. (c) The cumulative amount of LicoA percutaneous penetration. (d) The fluorescence map of the skin after percutaneous penetration. ($n=6$; * $p < 0.05$, ** $p < 0.01$ and *** $p < 0.001$).

3.3 Cell viability and whitening effect of supramolecular BR-LicoA-VE

After co-incubation of supramolecular BR-LicoA-VE with melanocytes for 72 h (Figure 3a), it was found that at a concentration of 0.00195%, the cell viability exceeded 90%, indicating that supramolecular BR-LicoA-VE was safe. The supramolecular BR-LicoA-VE can inhibit the production of melanin (Figure 3b), effectively combating skin exposed to excessive pigmentation and exhibiting outstanding whitening effects. Based on the 3D melanin model (MelaKutis®), compared with the control group, the apparent chromaticity of supramolecular BR-LicoA-VE significantly turned white at a concentration of 0.00195% (v/v) (Figure 3c), and the apparent brightness (L^* value) significantly increased with an improvement rate of 10.78% (Figure 3e). Melanin was transferred through dendrites like keratinocytes, and then with the loss of keratinocytes (Figure 3f), the content of melanin decreased significantly, and the inhibition rate was 30.45% (Figure 3d). Based on melanocytes, compared with the control group, the melanin content of supramolecular BR-LicoA-VE significantly decreased at a concentration of 0.00195% (v/v), with an inhibition rate of 30.55% (Figure 3g), a significant increase in tyrosinase activity inhibition rate, and a tyrosinase activity inhibition rate of 59.90% (Figure 3h). Therefore, it indicates that at this concentration, supramolecular BR-LicoA-VE was superior to the physical mixing group can improve apparent chromaticity, enhance apparent brightness (L^* value), inhibit melanin synthesis, inhibit tyrosinase activity, and have whitening effects on the sample [19].

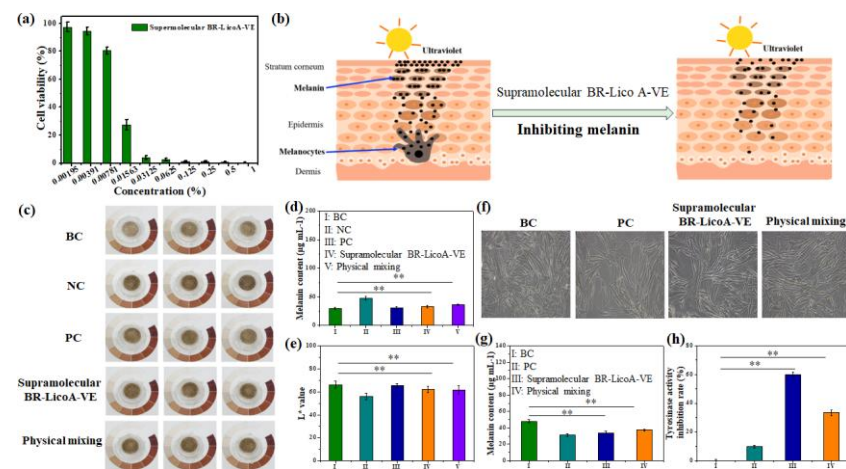


Figure 3. Cell viability and whitening effect of supramolecular BR-LicoA-VE. (a) Activity map of supramolecular BR-LicoA-VE on black cells. (b) Schematic diagram of supramolecular BR-LicoA-VE inhibiting melanocytes. (c) Schematic diagram of the apparent chromaticity, (d) melanin content, and (e) apparent brightness value of supramolecular BR-LicoA-VE on a 3D melanin model (MelaKutis®). (f) The dendritic cell diagram, (g) melanin content, and (h) tyrosinase inhibition rate of supramolecular BR-LicoA-VE on melanocytes. (n=3; * $p < 0.05$, ** $p < 0.01$, and *** $p < 0.001$).

3.4 The binding of supramolecular BR-LicoA-VE to proteins

TYR is the most widely studied target for inhibiting melanin production [6]. The docking results between BR and the TYR are shown in Figures 4 (a, b), the oxygen atom of the hydroxyl group on BR and the nitrogen atom of the His263 amino acid form hydrogen bonds and coordination bonds with Cu ions. The docking results of supramolecular BR-LicoA-VE and TYR are shown in Figure 4 (c, d), supramolecular BR-LicoA-VE can form two sets of hydrogen bonds with the His76 (A) and Arg108 (E) amino acids surrounding the pocket [20]. Similarly, the docking results of supramolecular BR-LicoA-VE and ET-1 protein molecules are shown in Figures 4 (e-h), it can be observed that supramolecular BR-LicoA-VE can form hydrogen bonds with the Arg96 amino acids surrounding the pocket. In addition, these results indicated that supramolecular BR-LicoA-VE inhibition of melanin production in cells was achieved by suppressing the expression of melanin-related proteins such as TYR, ET-1, mTOR, and MITF. Therefore, supramolecular technology provides a new approach to whitening and skincare.

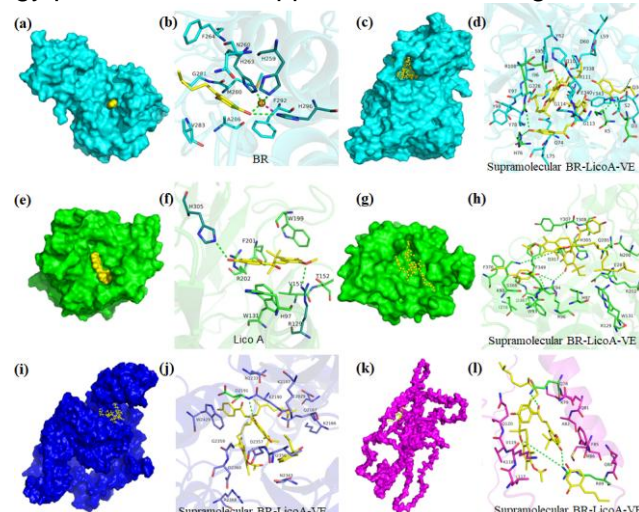


Figure 4. The binding of supramolecular BR-LicoA-VE to proteins. (a) The position of BR in the three-dimensional structure of TYR protein, (b) the three-dimensional binding mode diagram of BR with tyrosine TYR (green dashed line represents hydrogen bonding), (c) the position of supramolecular BR-LicoA-VE in the three-dimensional structure of TYR protein, (d) the three-dimensional binding mode diagram of supramolecular BR-LicoA-VE with TYR protein. (e) The position of LicoA in the three-dimensional structure of ET1 protein, (f) the three-dimensional binding mode diagram of LicoA with ET1 protein, (g) the position of supramolecular BR-LicoA-VE in the three-dimensional structure of ET1 protein, (h) the three-dimensional binding mode diagram of supramolecular BR-LicoA-VE with ET1 protein. (i) the position of supramolecular BR-LicoA-VE in the three-dimensional structure of mTOR protein, and (j) the three-dimensional binding mode diagram of supramolecular BR-LicoA-VE with mTOR protein (green dashed line represents hydrogen bonding). (k) The position of supramolecular BR-LicoA-VE in the three-dimensional structure of MITF protein, and (l) three-dimensional binding mode diagram of supramolecular BR-LicoA-VE with MITF protein.

3.5 Safety evaluation

The patch test results showed that there were 0 skin adverse reactions among the 34 subjects, indicating that the product had no skin adverse reactions to the human skin. In the 4-week clinical study, 0 subjects had local redness, itching, tingling, erythema, wheal, edema, or systemic skin adverse reactions. It showed that the products tested were mild overall.

3.6 Evaluation of the whitening, soothing, and repairing effects

The skin melanin index (MI) content was decreased by 3.49% after 14 days and by 4.35% after 28 days of using supramolecular BR-LicoA-VE formula (Figure 5a). The individual type angle (ITA°) was significantly increased by 7.35% after 14 days, and the ITA° was significantly increased by 8.95% after 28 days (Figure 5b). Compared with the placebo group, there was a significant difference at 28 days, indicating that supramolecular BR-LicoA-VE formula has whitening effect (Figures 5e,f). The erythema index (EI) content was decreased by 5.21% after 14 days, and the EI was significantly decreased by 16.31% after 28 days (Figure 5c), indicating that supramolecular BR-LicoA-VE formula has soothing effect. The transdermal water loss (TEWL) was significantly decreased by 11.98% after 14 days, and the TEWL was significantly decreased by 16.35% after 28 days (Figure 5d), indicating that supramolecular BR-LicoA-VE formula has repairing effect. Similarly, after using BR for 14 days, the skin MI increased by 4.19%, the ITA° significantly increased by 7.93%, the EI decreased by 5.00%, and the TEWL rate significantly decreased by 18.36%. After using BR for 28 days, the MI increased by 4.85%, the ITA° increased by 5.49%, the EI decreased by 11.23%, and the TEWL significantly decreased by 21.07%, so BR formula has a repairing effect. After using phenylethyl resorcinol (PR, 377) for 14 days, the skin MI increased by 1.34%, the ITA° skin was significantly increased by 10.04% (Compared with the placebo group, there was a significant difference at 28 days), the EI was decreased by 4.18%, and the TEWL was decreased by 7.22%. After 28 days of use, the skin MI was decreased by 3.05%, the ITA° was increased by 6.71% (compared with the placebo group, there was a significant difference at 14 and 28 days), the EI was significantly decreased by 10.17%, and the TEWL was significantly decreased by 16.49%. So PR formula has whitening, soothing and repairing effects. This set of results indicated that the whitening effect of supramolecular BR-LicoA-VE formula was better than that of single BR and PR [21, 22].

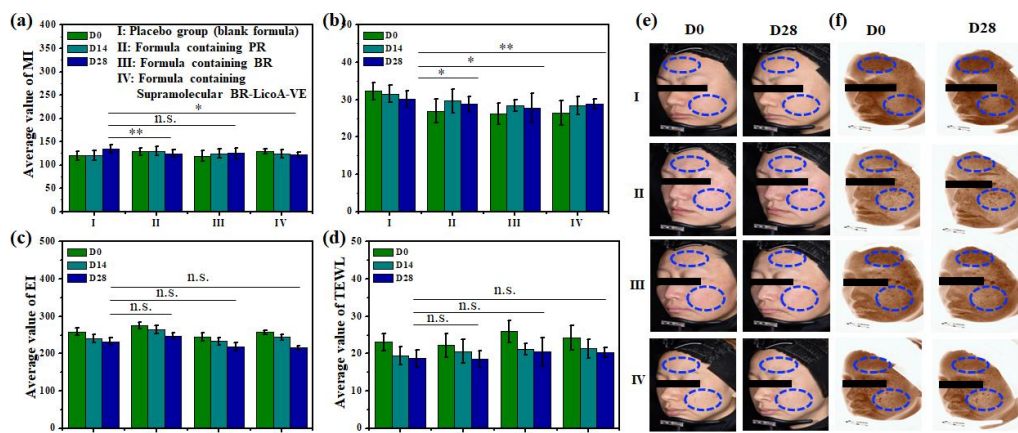


Figure 5. Evaluation of the whitening, soothing, and repairing effects of formula containing supramolecular BR-LicoA-VE. (a) MI value, (b) ITA° value, (c) EI value, (d) positive white light diagram and (f) brown spot diagram of the skin after 0, 14, 28 days of use of the sample. (n=47; * $p < 0.05$, ** $p < 0.01$, and *** $p < 0.001$).

4. Discussion

In this study, we aimed to study the whitening effect of supramolecular BR-LicoA-VE. Based on our hypothesis, we found that supramolecules can significantly enhance the whitening effect of 577, reduce irritation and improve skin permeability. This finding was consistent with the previous proof that supramolecules enhance the penetration of functional components. However, our results also show that the whitening effect of supramolecular BR-LicoA-VE was better than that of single 577 and 377. This finding may be of great significance in the field of whitening.

5. Conclusion

Supramolecular BR-LicoA-VE was successfully constructed through intermolecular forces, which significantly improved the transdermal absorption and stability of the active ingredient. The supramolecular BR-LicoA-VE can inhibit the tyrosinase activity of melanocytes and reduce melanin content and enhancing the skin brightness, better than the physically mixing control group. In addition, the formula containing supramolecular BR-LicoA-VE showed improvement in skin brightness properties and tendency for soothing skin redness via clinical trials, better than 577 and 377 group. In conclusion, transdermal co-delivery nanocarrier technology of supramolecular BR-LicoA-VE can achieve coordinated enhancement of skin whitening efficacy components with different mechanisms of action, high skin permeability, and no skin irradiation.

Acknowledgments

This work was supported by the National Natural Science Foundation of China (82073018, 21703218), the Shenzhen Science and Technology Innovation Committee (JCYJ20180507183907224).

References

- [1]. D. I. S. P. Resende, M. S. Ferreira, J. M. S. Lobo, et al. Skin depigmenting agents in anti-aging cosmetics: A medicinal perspective on emerging ingredients. *Appl. Sci.*, 2022, 12(2), 775-789.
- [2]. F. A. S. Addor. Beyond photoaging: additional factors involved in the process of skin aging. *Clin. Cosmet. Investig. Dermatol.*, 2018, 11, 437-443.
- [3]. P. P. Centeno, V. Pavet, R. Marais. The journey from melanocytes to melanoma. *Nat. Rev. Cancer*, 2023, 23(6), 372-390.

- [4]. F. F. Wang, W. J. Ma, D. J. Fan, *et al.* The biochemistry of melanogenesis: an insight into the function and mechanism of melanogenesis-related proteins. *Front. Mol. Biosci.*, 2024, 11, 1440187-1440201.
- [5]. Y. D. Wang, L. S. Han, G. Y. Li, *et al.* A comparative study of the chemical composition and skincare activities of red and yellow ginseng berries. *Molecules* 2024, 29(20), 4962-4977.
- [6]. H. Nakamura, M. Fukuda. Establishment of a synchronized tyrosinase transport system revealed a role of Tyrp1 in efficient melanogenesis by promoting tyrosinase targeting to melanosomes. *Sci. Rep.*, 2024, 14(1), 2529-2539.
- [7]. W. H. Shao, H. M. Ren, M. S. Yin, *et al.* Enhanced stability and reduced irritation of 4-n-butylresorcinol via nanoemulsion formulation: Implications for skin pigmentation treatment. *Eur. J. Med. Chem.*, 2024, 279, 116867-116877.
- [8]. Z. X. Wang, Y. Q. Xue, Z. M. Zhu, *et al.* Quantitative structure-activity relationship of enhancers of licochalcone A and glabridin release and permeation enhancement from carbomer hydrogel. *Pharmaceutics*, 2022, 14(2), 262-283.
- [9]. A. W. Lee, C. C. Hsu, Y. Z. Liu, *et al.* Supermolecules of poly(N-isopropylacrylamide) complexating Herring sperm DNA with bio-multiple hydrogen bonding. *Colloids Surf. B Biointerfaces*, 2016, 148, 422-430.
- [10]. A. Wishard, B. C. Gibb. Dynamic light scattering—an all-purpose guide for the supramolecular chemist. *Supramol. Chem.*, 2019, 31(9), 608-615.
- [11]. B. B. Lu, Y. Y. Bo, M. J. Yi, *et al.* Enhancing the solubility and transdermal delivery of drugs using ionic liquid-in-oil microemulsions. *Adv. Funct. Mater.*, 2021, 31(34), 2102794-2102805.
- [12]. T. Lu, Q. Chen, Interaction region indicator: A simple real space function clearly revealing both chemical bonds and weak interactions. *ChemRxiv*, 2021, 1(5), 231-239.
- [13]. B. B. Lu, S. R. Zhao, J. C. Zhang, *et al.* Anti-inflammatory and antioxidant effects on skin based on supramolecular hyaluronic acid-ectoin. *J. Mater. Chem. B*, 2024, 12(34), 8408-8419.
- [14]. B. B. Lu, Y. X. Zhong, J. L. Zhang, *et al.* Curcumin-based ionic liquid hydrogel for topical transdermal delivery of curcumin to improve its therapeutic effect on the psoriasis mouse model. *ACS Appl. Mater. Interfaces*, 2024, 16(14), 17080-17091.
- [15]. B. J. Zhou, S. Y. Liu, H. M. Yin, *et al.* Development of gliclazide ionic liquid and the transdermal patches: An effective and noninvasive sustained release formulation to achieve hypoglycemic effects. *Eur. J. Pharm. Sci.*, 2021, 164, 105915-105971.
- [16]. B. B. Lu, J. L. Zhang, J. H. Zhang. Enhancing transdermal delivery of curcumin-based ionic liquid liposomes for application in psoriasis. *ACS Appl. Bio. Mater.*, 2023, 6(12), 5864-5873.
- [17]. L. J. Ding, J. Yang, K. R. Yin, *et al.* The spatial arrangement of astaxanthin in bilayers greatly influenced the structural stability of DPPC liposomes. *Colloids Surf. B Biointerfaces*, 2022, 212, 112383-112391.
- [18]. Z. X. Wang, Y. Q. Xue, T. T. Chen, *et al.* Glycyrrhiza acid micelles loaded with licochalcone A for topical delivery: Co-penetration and anti-melanogenic effect. *Eur. J. Pharm. Sci.*, 2021, 167, 106029-106041.
- [19]. G. Aceto, L. D. Muzio, R. D. Lorenzo, *et al.* Dual delivery of ginger oil and hexylresorcinol with lipid nanoparticles for the effective treatment of cutaneous hyperpigmentation. *J. Drug Deliv. Sci. Technol.*, 2013, 87, 104790-104799.
- [20]. J. Kim, S. C. Hong, E. H. Lee, *et al.* Preventive effect of *M. cochinchinensis* on melanogenesis via tyrosinase activity inhibition and p-PKC signaling in Melan-A cell. *Nutrients*, 2021, 13(11), 3894-3904.

- [21]. Z. X. Wang, Y. Q. Xue, Q. F. Zeng, *et al.* Glycyrrhiza acid-Licochalcone A complexes for enhanced bioavailability and anti-melanogenic effect of Licochalcone A: cellular uptake and in vitro experiments. *J. Drug Deliv. Sci. Technol.*, 2022, 68, 103037-103046.
- [22]. B. S. Kim, Y. G. Na, J. H. Choi, *et al.* The improvement of skin whitening of phenylethyl resorcinol by nanostructured lipid carriers. *Nanomaterials*, 2017, 7(9), 241-250.